52nd IEEE Conference on Decision and Control
December 10-13, 2013. Florence, Italy

Voltage Stabilization in Microgrids via Quadratic Droop Control

John W. Simpson-Porco, Florian Dörfler, and Francesco Bullo

***Abstract*— Motivated by the growing interest in energy technology and smart grid architectures, we consider the problem of voltage stability and reactive power balancing in low-voltage electrical networks equipped with DC/AC inverters ("microgrids"). It is generally believed that high-voltage equilibria of such networks are stable, but the locations of these equilibria are unknown, as is the critical network load where stability is lost. Inspired by the "control by interconnection" paradigm developed for port-Hamiltonian systems, we propose a novel droop-like inverter controller which is quadratic in the local voltage magnitude. Remarkably, under this controller the closed-loop network is again a well-posed electrical circuit. We find that the equilibria of the quadratic droop-controlled network are in exact correspondence with the solutions of a reduced power flow equation. For general network topologies, we study some simple yet insightful solutions of this equation, and for the frequently-encountered case of a parallel microgrid, we present a concise and closed-form condition for the existence of an exponentially stable high-voltage network equilibrium. Our condition establishes the existence of a critical inductive load for the network, which depends only on the network topology, admittances, and controller gains. We compare and contrast our design with the conventional droop controller, investigate the relationship between the two, and validate the robustness of our design through simulation.**

I. Introduction

Due to environmental and social factors, and the rapidly expanding integration of low voltage small-scale renewable energy sources, the present centralized wide-area electric power transmission paradigm is evolving towards a more distributed future. As a bridge between high-voltage transmission and low-voltage distributed generation, the concept of a *microgrid* has recently gained significant traction [1]. Microgrids are low-voltage electrical distribution networks, heterogeneously composed of distributed generation, storage, load, and managed autonomously from the larger primary network. Microgrids are able to connect to the wide area electric power system through a "Point of Common Coupling", but are also able to "island" themselves and operate independently [2], [3]. Energy generation within a microgrid can be highly heterogeneous, including photovoltaic, wind, geothermal, micro-turbines, etc. Many of these sources generate either variable frequency AC power or DC power, and are interfaced with a synchronous AC grid via power electronic DC/AC *inverters*. In islanded operation, it is through these inverters that actions must be taken to ensure synchronization, voltage stability, power balance and load sharing in the network [1].

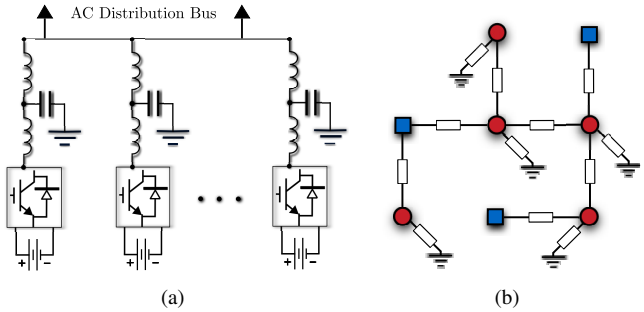

Fig. 1. (a) Schematic of a "parallel" microgrid, in which several inverters supply power to a distribution bus (effectively a single load) (b) A simple non-parallel microgrid consisting of five loads ● and three inverters ■.

A. Literature Review

The so-called *droop controllers* (and their derivatives) have been used with some success to achieve these tasks, see [1]–[8]. Despite forming the foundation for the networked operation of inverters (Figure 1), droop-controlled networks of inverters and loads have only recently been subject to a rigorous analysis. In [9], we provided an exact nonlinear analysis of the "ω-P" droop control law, which is used for frequency synchronization and active power balancing (see Section II-B). While the emphasis in the literature has been placed on the analysis of synchronization and active power, the lower voltage levels and uncompensated loads in microgrids can cause voltage magnitudes to fall to dangerously low levels, leading to voltage instability and collapse [10]. At the transmission level, these phenomena have received increasing attention after recent voltage instability induced blackouts in Scandinavia (2003), Canada/USA (2003), and Greece (2004) [11]. Indeed, the U.S. Department of Energy has recently invested significant resources studying strategies for reactive power support and the shaping of network voltage profiles [12]. This leads immediately to the problem complementary to synchronization and active power balancing, namely voltage stabilization and reactive power balancing. Over the 20 years since its introduction in [13], the "E-Q" voltage-droop controller (Section II-B) has become the key tool used for these tasks.

The widespread deployment and practical utility of the E-Q controller has led to several attempts at analysis [14], [15]. However, these attempts have met with remarkably little success. To our knowledge, the only provably correct conditions for stability were presented in [15]. Unfortunately,

This work was supported in part by the National Science Foundation NSF CNS-1135819 and by the National Science and Engineering Research Council of Canada. We wish to thank I. Dobson and I. Hiskens for fruitful conversations on the topic of reactive load flow.

J. W. Simpson-Porco and F. Bullo are with the Center for Control, Dynamical Systems and Computation, University of California Santa Barbara. Email: {johnwsimpsonporco,bullo}@engineering.ucsb.edu. F. Dörfler is with the Department of Electrical Engineering, University of California Los Angeles. Email: dorfler@seas.ucla.edu.

the conditions in [15] are extremely conservative, and hold only for the all-to-all networks of inverters which appear in network-reduced models. Analyses which *begin* from network-reduced models — models in which the load nodes are eliminated from the network — are inherently unable to address the heart of the problem; the voltage levels seen at the load terminals of the true physical network. Said differently, the literature offers no guidance on the foundational issue of operating point feasibility. That is, the existence and locations of equilibria for the network. This large gap of knowledge regarding E-Q controlled networks means that precise reactive loading limits and security margins are inherently unknown, making system monitoring and non-conservative operation difficult.

B. High-Voltage Stability & Critical Inductive Loading

Classic intuition developed in power systems is that inductive loading distorts the spatial voltage profile in a network by dragging down the voltage magnitudes at inductively loaded nodes. Moreover, it is generally accepted that high-voltage (low loss) equilibria of such networks are stable, while low-voltage (high loss) equilibria are unstable [11]. Taken together, these rules of thumb suggest the existence of a *critical inductive load* which depends on the network under consideration. If the total load is less inductive than this critical value, the network voltage profile will be sufficiently homogeneous and a stable high-voltage equilibrium will exist. The classic works [16], [17] give some conservative estimates of this critical load in transmission networks. A fundamental outstanding problem regarding the voltage stability of droop-controlled microgrids is therefore to relate the existence of stable high-voltage equilibria to the network topology, line admittances, loads, and controller gains, and to determine the exact locations of the equilibria should any exist.

C. Contributions

There are four main contributions of this paper. First, in Section III we present a novel alternative to the conventional voltage-droop controller, which we refer to as the *quadratic droop controller*. In contrast with the conventional controller — the design of which is motivated by the local, linear behavior of power flow near a steady-state operating point — our proposed design is inspired by the "control by interconnection" approach from port-Hamiltonian systems [18]. We find that the analysis of the network is greatly simplified by designing a controller which preserves the quadratic structure of the AC power flow equations in closed-loop. In particular, we show that the equilibria of the network when controlled by our quadratic droop controller are in exact correspondence with the solutions of a reduced power flow equation (RPFE). For general network topologies, we solve our RPFE for two insightful load profiles: the case of no loading, and the case of ZI loads; see Section II-A for background on load models).

Second, in Section IV we consider in detail the common and practically relevant case of a parallel microgrid (Figure 1(a)). By explicitly solving our RPFE we provide a necessary and sufficient condition on the network load for the existence of a locally exponentially stable high-voltage equilibrium point. Confirming classic intuition, our condition establishes the existence of a critical inductive load for the network, which depends only on the network topology, admittances, inverter set point voltages, and controller gains. The condition succinctly states that the network load must be less inductive than this critical value. In addition, we study the (in)stability properties of the complementary low-voltage equilibrium point, and in doing so provide a quite complete picture of the network state space.

As a third contribution, in Section V we use the results we derive for the quadratic droop controller to draw a correspondence between the equilibria of the quadratic droop-controlled network and the equilibria of the same network when controlled by the conventional droop controller. While not a bidirectional correspondence, in doing so we provide the first characterization of the network equilibrium points (and their stability properties) under the conventional voltage-droop controller.

Fourth and finally, in Section VI we demonstrate the robustness of our design by exploring through simulation a scenario beyond the scope of our theoretical results. In particular, we examine the performance of the controller in a modified version of the mixed resisitve/inductive IEEE 37 bus distribution network. Proofs of all results are deferred to a journal publication to follow.

D. Preliminaries and Notation

Sets, vectors and functions: Given a finite set $\mathcal{V}$, let $|\mathcal{V}|$ denote its cardinality. The set $\mathbb{S}$ is the unit circle. We let $\mathbb{R}$ (resp. $\mathbb{R}_{>0}$) denote the set of real (resp. strictly positive real) numbers. Similarly, given $\mathcal{D} \subset \mathbb{R}^n$, let $\mathcal{D}_{>0} \triangleq \mathcal{D} \cap \mathbb{R}^n_{>0}$ be the restriction of $\mathcal{D}$ to the positive orthant. Given an index set $\mathcal{I}$ and a real valued 1D-array $\{x_1, \ldots, x_{|\mathcal{I}|}\}$, $\{x_i\}_{i\in\mathcal{I}}$, or simply $x \in \mathbb{R}^{|\mathcal{I}|}$ is the associated vector, with $[x] \in \mathbb{R}^{|\mathcal{I}|\times|\mathcal{I}|}$ being the associated diagonal matrix. Given $x, y \in \mathbb{R}^n$, we write $x \gg y$ if $x_i > y_i$ for each $i \in \{1, \ldots, n\}$. Throughout, $\mathbf{1}_n$ and $\mathbf{0}_n$ are the n-dimensional vectors of unit and zero entries, with $\mathbf{0}$ being a matrix of all zeros of appropriate dimensions. A matrix $W \in \mathbb{R}^{n\times m}$ is row-stochastic if its elements are nonnegative and $W\mathbf{1}_m = \mathbf{1}_n$.

Algebraic graph theory: Given an undirected, connected, and weighted graph $G(\mathcal{V}, \mathcal{E}, A)$ induced by the symmetric, nonnegative and irreducible *adjacency matrix* $A \in \mathbb{R}^{n\times n}$, we define the *nodal degree* by $\deg_i = \sum_{j=1}^n a_{ij}$. The *Laplacian matrix* $L \in \mathbb{R}^{n\times n}$ is defined by $L = \operatorname{diag}(\{\deg_i\}_{i=1}^n) - A$.

Differential-algebraic systems: Consider the differential-algebraic system

$$\dot{x} = f(x, y)\,, \quad \mathbf{0}_m = g(x, y)\,, \tag{1}$$

where $x \in \mathbb{R}^n$, $y \in \mathbb{R}^m$, and $f : \mathbb{R}^{n+m} \to \mathbb{R}^n$, $g : \mathbb{R}^{n+m} \to \mathbb{R}^m$ are sufficiently smooth. Let $\mathcal{M} = \{(x, y) \in \mathbb{R}^{n+m} \mid \mathbf{0}_m = g(x, y)\}$ be the constraint set of (1), and define the *singular set* $\mathcal{S}$ of $g(x, y)$ by

$$\mathcal{S} \triangleq \left\{ (x, y) \in \mathcal{M} \;\middle|\; \det \frac{\partial g}{\partial y} = 0 \right\}. \tag{2}$$

The singular set $\mathcal{S}$ decomposes $\mathcal{M}$ into open sets $\mathcal{M}_i$ where $\det \frac{\partial g}{\partial y}$ is sign-definite and such that $\mathcal{M} = \mathcal{S} \cup (\cup_i \mathcal{M}_i)$. Components $\mathcal{M}_i$ with $\det \frac{\partial g}{\partial y} < 0$ (resp. $\det \frac{\partial g}{\partial y} > 0$) are called *stable* (resp. *unstable*) [19].

II. Problem Setup

We briefly review the classic theory of AC power flow and recall the definitions for the conventional droop controllers.

A. Review of Microgrids and AC Circuits

Throughout this work we adopt the standard model of a microgrid as synchronous linear circuit with admittance matrix $Y \in \mathbb{C}^{n\times n}$. The associated connected, undirected, and complex-weighted graph is $G(\mathcal{V}, \mathcal{E}, A)$ with node set (or buses) $\mathcal{V} = \{1, \dots, n\}$, edge set (or branches) $\mathcal{E} \subset \mathcal{V} \times \mathcal{V}$, and symmetric edge weights (or admittances) $a_{ij} = -Y_{ij} = -Y_{ji} \in \mathbb{C}$ for every branch $\{i, j\} \in \mathcal{E}$. We partition the set of buses as $\mathcal{V} = \mathcal{V}_L \cup \mathcal{V}_I$, corresponding to the loads and inverters. To each bus $i \in \mathcal{V}$, we associate an electrical power injection $S_{\mathrm{e},i} = P_{\mathrm{e},i} + \sqrt{-1}Q_{\mathrm{e},i} \in \mathbb{C}$ and a phasor voltage variable $V_i = E_i e^{\sqrt{-1}\theta_i}$ corresponding to the magnitude $E_i > 0$ and the phase shift $\theta_i \in \mathbb{S}$ of a harmonic solution to the AC power flow equations. The linear current-balance equations are $I = YV$, where $I \in \mathbb{C}^n$ and $V \in \mathbb{C}^n$ the vectors of nodal current injections and voltages. The complex vector of nodal electrical power injections is then given by $S_{\mathrm{e}} = [V](YV)^*$. For inductive lines, the admittance matrix $Y \in \mathbb{C}^{n\times n}$ is purely imaginary, and the active/reactive nodal electrical power injections are given by

$$P_{\mathrm{e},i} = \sum\nolimits_{j=1}^{n} \mathfrak{Im}(Y_{ij}) E_i E_j \sin(\theta_i - \theta_j)\,, \qquad i \in \mathcal{V}\,, \quad \text{(3a)}$$

$$Q_{\mathrm{e},i} = -\sum\nolimits_{j=1}^{n} \mathfrak{Im}(Y_{ij}) E_i E_j \cos(\theta_i - \theta_j)\,, \quad i \in \mathcal{V}. \quad \text{(3b)}$$

Strictly for simplicity of both presentation and mathematical development, we will work under the standard *decoupling approximation*, where $\theta_i - \theta_j \approx 0$ and hence $\cos(\theta_i - \theta_j) \approx 1$ for each $\{i, j\} \in \mathcal{E}$; see [8], [20]. This assumption can be relaxed to nonzero power angles $\theta_i - \theta_j \neq 0$ at the cost of a more complicated and less elegant formulation, but doing so adds little in terms of the presentation herein. Under this decoupling assumption, the reactive power flow (3b) can be written in compact vector notation as

$$Q_{\mathrm{e}} = [E]LE\,, \tag{4}$$

where $E = \{E_i\}_{i\in\mathcal{V}}$, and the (negative) susceptance matrix $L \triangleq -\mathfrak{Im}(Y) \in \mathbb{R}^{n\times n}$ is a Laplacian matrix. If the network is primarily resistive instead of inductive, Q can be replaced by P and all stability results presented herein go through [14]. For load modeling, throughout the paper we consider subsets of standard ZIP loads, which take the form $Q_i(E_i) = a_{i1}E_i^2 + a_{i2}E_i + a_{i3}$ [20], [21]. Here, the real coefficients a_{i1}, a_{i2}, and a_{i3} correspond to the constant-impedance, constant-current, and constant-power portions of the load. As is standard in the microgrid literature, we model an inverter as a controllable voltage source behind a reactance. This model is *widely adopted* among experimentalists in the microgrid field. Further modeling explanation can be found in [3], [22], [23] and the references therein.

B. Review of Conventional Droop Control

The *conventional droop controllers* are the foundational techniques for primary control (synchronization, voltage stability and power balancing) in islanded microgrids. The controllers are heuristics based on the classic active/reactive decoupling assumption for small power angles and non-mixed line conditions, see [1], [2], [4], [6], [7], [13], [14], [24]–[27]. For the case of inductive lines, the droop controllers specify both the inverter frequencies ω_i and output voltage magnitudes E_i by [3, Chapter 19]

$$\omega_i = \omega^* - m_i P_{\mathrm{e},i}\,, \quad i \in \mathcal{V}_I\,, \tag{5a}$$

$$E_i = E_i^* - n_i Q_{\mathrm{e},i}\,, \quad i \in \mathcal{V}_I, \tag{5b}$$

where $\omega^* > 0$ is the nominal network frequency, $E_i^* > 0$ is the nominal voltage for the i^{th} inverter, and $P_{\mathrm{e},i}$ (resp. $Q_{\mathrm{e},i}$) is the *measured* active (resp. reactive) power injection*. The controller gains $m_i, n_i > 0$ are referred to as droop coefficients. See [9] for a detailed analysis of the control law (5a). From (5b), it is clear that if an inverter injects a non-zero amount of reactive power $Q_{\mathrm{e},i}$, its voltage will deviate from E_i^*. For easy comparison with our design, it will be convenient to add an integral channel to the controller (5b) yielding the first-order *conventional droop controller*

$$\tau_i \dot{E}_i = -\widetilde{C}_i(E_i - E_i^*) - Q_{\mathrm{e},i}\,, \tag{6}$$

where $\tau_i > 0$ and $\widetilde{C}_i \triangleq n_i^{-1}$. Note that solutions of (5b) correspond to steady states of (6).

III. Quadratic Droop Control for Voltage Stabilization

While the droop controller (6) is simple and intuitive, it is based on the linear behavior of AC power flow around a stable equilibrium, and cannot account for the quadratic and asymmetric nature of reactive power flow in inductive networks. In this section we propose a physically motivated modification of the conventional voltage-droop controller (6). In place of (6), consider instead the *quadratic droop controller*

$$\boxed{\tau_i \dot{E}_i = -C_i E_i (E_i - E_i^*) - Q_{\mathrm{e},i}\,, \quad i \in \mathcal{V}_I,} \tag{7}$$

where $\tau_i, C_i, E_i^* > 0$ are control parameters. Note that the gain on the local feedback term is no longer constant but scales with the local inverter voltage E_i. For loads $\{Q_i\}_{i\in\mathcal{V}_L}$, we must also satisfy the $|\mathcal{V}_L|$ reactive power balance equations

$$0 = Q_i - Q_{\mathrm{e},i}\,, \quad i \in \mathcal{V}_L\,. \tag{8}$$

Combining (7), (8), and (4), the closed-loop differential-algebraic dynamics are given in vector notation by

$$\begin{pmatrix} \mathbf{0}_{|\mathcal{V}_L|} \\ \tau_I \dot{E}_I \end{pmatrix} = \begin{pmatrix} Q_L \\ C_I[E_I](E_I^* - E_I) \end{pmatrix} - [E]LE\,, \tag{9}$$

where $\tau_I = [\{\tau_i\}_{i\in\mathcal{V}_I}]$, $C_I = [\{C_i\}_{i\in\mathcal{V}_I}]$, $E_I = \{E_i\}_{i\in\mathcal{V}_I}$, $E_I^* = \{E_i^*\}_{i\in\mathcal{V}_I}$ and $Q_L = \{Q_i\}_{i\in\mathcal{V}_L}$. The closed-loop dynamics (9) highlight the competition in the network between

*See [3], [22] for details regarding estimation of active/reactive powers.

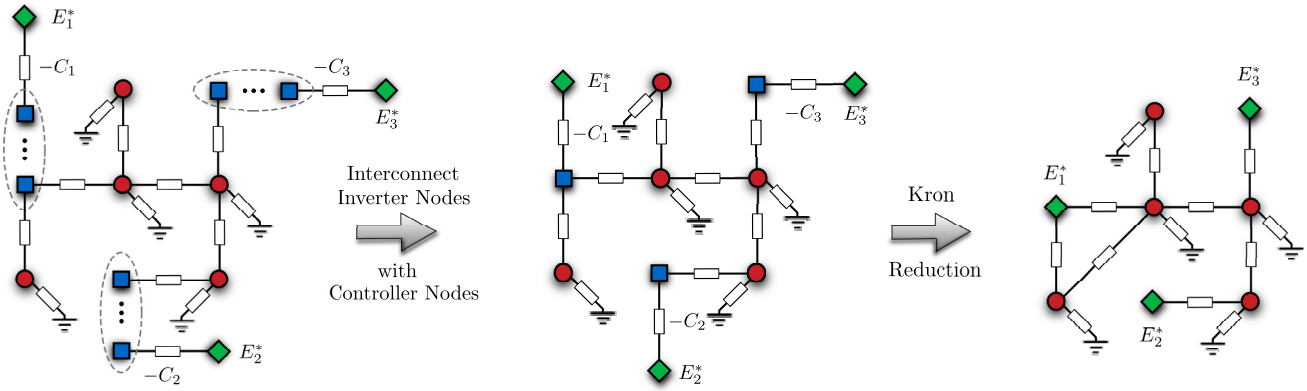

Fig. 2. Diagram showing network augmentation and reduction. First, each inverter node ■ of the network in Figure 1(b) is interconnected with a two-node controller circuit, consisting of an inverter node ■ and fictitious node ◆ at constant voltage E_i^*. In Theorem 3.1, the inverter nodes are eliminated via Kron reduction, leaving a reduced network with only fixed voltage nodes ◆ and load nodes ●.

the driving terms in parentheses, which attempt to distort the network voltage profile, and the homogenizing effect of the network through the (nonlinear) consensus $[E]LE$.

Remark 1: **(Interpretation of Quadratic Droop Controller).** In analogy with feedback strategies used in the study of port-Hamiltonian systems [18], the design (7) can be interpreted as *control by interconnection*, where we interconnect the physical electrical network with fictitious controller circuits at the inverter nodes $i \in \mathcal{V}_I$ [28]. Indeed, consider

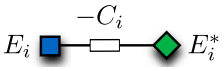

Fig. 3. Linear circuit representation of the quadratic droop controller (7).

the two-node circuit of Figure 3, where the first node has variable voltage E_i and is connected via a susceptance $-C_i$ to the second node at fixed voltage E_i^*. The current-voltage relations for this circuit take the form

$$\begin{pmatrix} I_i \\ I_i^* \end{pmatrix} = \begin{pmatrix} C_i & -C_i \\ -C_i & C_i \end{pmatrix} \begin{pmatrix} E_i \\ E_i^* \end{pmatrix}, \tag{10}$$

where I_i (resp. I_i^*) is the extracted current† at the node with voltage E_i (resp. E_i^*). Now, let there be $|\mathcal{V}_I|$ of the two-node circuits in Figure 3. If we associate the variable-voltage nodes of these circuits with the inverter nodes of our original network (Figure 2) by imposing that the current injected into one must exit from the other, we obtain an augmented network with $n+|\mathcal{V}_I|$ nodes, and in vector notation the current-voltage relations in the new network take the form

$$\begin{pmatrix} I_L \\ \mathbf{0}_{|\mathcal{V}_I|} \\ I_I^* \end{pmatrix} = \begin{pmatrix} L_{LL} & L_{LI} & \mathbf{0} \\ L_{IL} & L_{II}+C_I & -C_I \\ \mathbf{0} & -C_I & C_I \end{pmatrix} \begin{pmatrix} E_L \\ E_I \\ E_I^* \end{pmatrix}, \tag{11}$$

where we have partitioned the nodal currents and voltage magnitudes in terms of the loads (I_L and E_L), inverters (I_I and E_I), and the fictitious controller nodes (I_I^* and E_I^*). In this augmented network, the inverters behave as interior nodes connecting the fictitious controller nodes to the loads, and do not sink or source power themselves. Left multiplying the first two blocks of equations in (11) by $[E]$ and noting that $[E_L]I_L = Q_L$, we immediately obtain the right hand side of (9). Thus, unlike the conventional droop controller (6), the quadratic droop controller preserves the structure of the network circuit equations in closed-loop. □

Remark 2: **(State Space of Network).** Let $\mathcal{M} \subset \mathbb{R}^n$ denote the $|\mathcal{V}_I|$-dimensional subset of $\mathbb{R}^n$ defined implicitly by the $|\mathcal{V}_L|$ algebraic equations in the closed-loop system (9). We consider (9) to be defined only on the intersection $\mathcal{M}_{>0} = \mathcal{M} \cap \mathbb{R}^n_{>0}$. Indeed, within the phasor modeling framework, each nodal voltage E_i represents a voltage *magnitude* and is intrinsically nonnegative. This choice of state space will simplify our analysis by excluding non-physical and short-circuit equilibria which would not occur in practice. □

A basic question regarding the closed-loop system (9) is the following: under what conditions on load, network topology, admittances, and controller gains does the differential-algebraic system (9) possess a locally exponentially stable equilibrium? Our first result exploits the homogeneous quadratic nature of the control law (7) to establish a correspondence between the equilibria of (9) and the solutions of a power flow equation for a reduced network.

Theorem 3.1: **(Reduced Power Flow Equation for Quadratic Droop Network).** Consider the closed-loop system (9) resulting from the quadratic droop controller (7). Partition the Laplacian matrix and nodal voltage variables according to loads and inverters as

$$L = \begin{pmatrix} L_{LL} & L_{LI} \\ L_{IL} & L_{II} \end{pmatrix}, \qquad E = (E_L, E_I)^T,$$

and define

$$L_{\text{red}} \triangleq L_{LL} - L_{LI}\left(C_I + L_{II}\right)^{-1} L_{IL} \in \mathbb{R}^{|\mathcal{V}_L|\times|\mathcal{V}_L|}, \tag{12}$$

$$W_1 \triangleq -L_{\text{red}}^{-1} L_{LI}\left(L_{II} + C_I\right)^{-1} C_I \in \mathbb{R}^{|\mathcal{V}_L|\times|\mathcal{V}_I|}, \tag{13}$$

†"Extracted" because $L = -\mathfrak{Im}(Y)$. Since we work under the decoupling assumption, these are technically the imaginary parts of the currents.

$$E^*_{\rm avg} \triangleq W_1 E^*_I \in \mathbb{R}^{|\mathcal{V}_L|}_{>0}\,, \tag{14}$$

$$W_2 \triangleq (L_{II}+C_I)^{-1}\begin{pmatrix}-L_{IL} & C_I\end{pmatrix} \in \mathbb{R}^{|\mathcal{V}_I|\times n}. \tag{15}$$

The following two statements are equivalent:

(i) **Original Network:** The network voltage vector $E = (E_L, E_I) \in \mathcal{M}_{>0}$ is an equilibrium point of (9);

(ii) **Reduced Network:** The load voltage vector $E_L \in \mathbb{R}^{|\mathcal{V}_L|}_{>0}$ solves the reduced power flow equation (RPFE)

$$Q_L = [E_L] L_{\rm red}(E_L - E^*_{\rm avg})\,, \tag{16}$$

and the inverter voltage vector is given by

$$E_I = W_2 \begin{pmatrix} E_L \\ E^*_I \end{pmatrix} \in \mathbb{R}^{|\mathcal{V}_I|}_{>0}\,. \tag{17}$$

Remark 3: **(Interpretation of Reduced Power Flow Equations).** Given the "control by interconnection" interpretation of the quadratic droop controller introduced in Remark 1, the RPFE (16) is straightforward to interpret. Eliminating the inverter voltages E_I from the augmented network current-voltage relations (11) through Kron reduction [29], one obtains the equivalent reduced representation

$$\begin{pmatrix} I_L \\ I^*_I \end{pmatrix} = \begin{pmatrix} L_{\rm red} & -L_{\rm red}W_1 \\ -W_1^T L_{\rm red} & C_I(L_{II}+C_I)^{-1}L_{II} \end{pmatrix} \begin{pmatrix} E_L \\ E^*_I \end{pmatrix}.$$

Left-multiplying the first equation by $[E_L]$ immediately yields (16). Hence, the RPFE (16) is exactly the reactive power balance equation $Q_L = [E_L]I_L$ in the reduced network at the load nodes $\mathcal{V}_L$, with current injections given by $I_L = L_{\rm red}(E_L - E^*_{\rm avg})$ (c.f. [21, Equation 2.10b]). The second line of equations can be thought of as determining the fictitious controller current injections once the first set are solved for E_L. This reduction process is shown in Figure 2. Note that while the number of nodes in the original network and in the reduced network are equal, the topologies are not necessarily the same [29, Theorem 3.4]. □

Theorem 3.1 immediately yields two insightful results.

Corollary 3.2: **(Exact Solution for Zero Load).** Consider the RPFE (16) for no load, i.e., $Q_L = \mathbf{0}_{|\mathcal{V}_L|}$. Then $E_L = E^*_{\rm avg}$ is the unique solution in $\mathbb{R}^{|\mathcal{V}_L|}_{>0}$.

It can be shown that W_1 is row-stochastic, and hence by (14) each component of $E^*_{\rm avg}$ is a convex combination of the inverter set points E^*_I. Thus, W_1 describes how the set point voltages are averaged by the network to produce the load terminal voltages under zero reactive loading. We note that this "baseline" voltage profile is non-uniform, due to the inhomogeneous inverter set point voltages. While (16) is difficult to solve for general ZIP loads, a simple and general result for combinations of constant-impedance/current ($a_{i3} = 0$) loads follows from Theorem 3.1.

Corollary 3.3: **(Exact Solution for ZI Loads).** Consider the RPFE (16) for ZI loads

$$Q_L = [E_L][b_{\rm shunt}]E_L + [E_L]I_{\rm shunt}\,, \tag{18}$$

where the constant-impedance loads are non-capacitive ($[b_{\rm shunt}] \in \mathbb{R}^{|\mathcal{V}_L|\times|\mathcal{V}_L|}$ is negative semidefinite) and the constant-current load vector $I_{\rm shunt} \in \mathbb{R}^{|\mathcal{V}_L|}$ satisfies $I_{\rm shunt} \gg -L_{\rm red}E^*_{\rm avg}$. Then the unique solution $E_L \in \mathbb{R}^{|\mathcal{V}_L|}_{>0}$ to (16) is given by

$$E_L = (L_{\rm red} - [b_{\rm shunt}])^{-1}(L_{\rm red}E^*_{\rm avg} + I_{\rm shunt})\,. \tag{19}$$

IV. Quadratic Droop Control for Parallel Microgrids

While complex in general, the RPFE (16) is particularly simple for the common class of *parallel microgrids*, which consist of a single load fed by multiple inverters in parallel (Figure 1(a)). In this section we let nodes $\mathcal{V}_I = \{1,\dots,n-1\}$ correspond to the inverter nodes, and let node $\mathcal{V}_L = \{0\}$ be the common connection point for a total of n nodes. In this case, the network Laplacian has the simple structure

$$L = \begin{pmatrix} \sum_{i=1}^{n-1}|b_{i0}| & -|b_{10}| & \cdots & -|b_{(n-1)0}| \\ -|b_{10}| & |b_{10}| & \cdots & 0 \\ \vdots & \vdots & \ddots & \vdots \\ -|b_{(n-1)0}| & 0 & \cdots & |b_{(n-1)0}| \end{pmatrix},$$

where $b_{i0} < 0$ is the susceptance between inverter $i \in \{1,\dots,n-1\}$ and the load (or distribution bus). In this case, the algebraic power flow equation (8) takes the form[‡]

$$h(E) \triangleq Q_0 - \sum_{j=1}^{n-1}|b_{j0}|E_0(E_0 - E_j) = 0\,. \tag{20}$$

Before studying the equilibria for this configuration, we examine closely the global structure of our constraint set $\mathcal{M} \triangleq \{E \in \mathbb{R}^n \mid h(E) = 0\}$ (see Figure 4).

Lemma 4.1: **(Topology of Constraint Set for Parallel Microgrid).** Consider the power balance equation (20) for a parallel microgrid, and define the *total susceptance magnitude* $b_{\rm tot} > 0$ and the *singular normal vector* $a \in \mathbb{R}^n$ by

$$b_{\rm tot} \triangleq \sum_{j=1}^{n-1}|b_{j0}|\,, \quad a \triangleq \left(-1\,,\, \frac{|b_{10}|}{2b_{\rm tot}}\,,\,\dots\,,\, \frac{|b_{(n-1)0}|}{2b_{\rm tot}}\right)^T,$$

with associated hyperplane

$$\mathcal{H} \triangleq \left\{E \in \mathbb{R}^n \,|\, a^T E = 0\right\}. \tag{21}$$

The following statements hold:

(i) **Singular Surface:** The singular surface $\mathcal{S}$ of the load power balance (20) is given by $\mathcal{S} = \mathcal{M} \cap \mathcal{H}$;

(ii) **Topology of State Space $\mathcal{M}_{>0}$:**

(a) If $Q_0 \geq 0$, there exists a unique stable component $\mathcal{M}^{\rm stable}$ of $\mathcal{M}$ such that $\mathcal{M}_{>0} = \mathcal{M}^{\rm stable}_{>0}$ is nonempty and simply connected;

(b) If $Q_0 < 0$, there exist unique stable and unstable components $\mathcal{M}^{\rm stable}$ (resp. $\mathcal{M}^{\rm unstable}$) of $\mathcal{M}$ such that $\mathcal{M}_{>0} = \mathcal{M}^{\rm stable}_{>0} \cup \mathcal{M}^{\rm unstable}_{>0} \cup \mathcal{S}_{>0}$, where all sets in the union are nonempty and simply connected.

Remark 4: **(Physically Measurable States).** It is argued in [19] that $\mathcal{M}^{\rm stable}_{>0}$ is the only physically observable portion

[‡]As "stiff" constant-power loads ($a_{i1} = a_{i2} = 0$) are the most interesting, we restrict ourselves to them in the sequel, and denote the load by Q_0. Our results for the parallel topology extend to general ZIP loads.

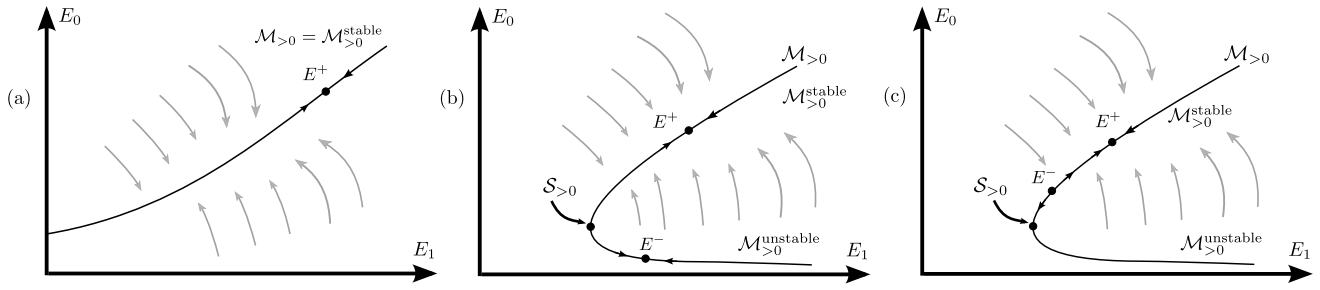

Fig. 4. Equilibrium locations for (a) $Q_0 > 0$, (b) $Q_0 \in]-Q_{\text{sing}}, 0[$, and (c) $Q_0 \in]-Q_{\text{crit}}, -Q_{\text{sing}}[$. Gray arrows represent the behavior of the associated singularly perturbed system (22) with parasitic term $\varepsilon \dot{E}_0$.

of the state space, in that if one performed measurements on the physical system in steady state, one would only ever obtain measurements on or near $\mathcal{M}^{\text{stable}}_{>0}$. The restriction to $\mathcal{M}_{>0}$ is clear from Remark 2. To understand the additional restriction to the stable component, consider instead of the load balance (20) an associated *singularly perturbed* system

$$\varepsilon \dot{E}_0 = h(E)\,, \tag{22}$$

where $\varepsilon > 0$. The additional term $\varepsilon \dot{E}_0$ could arise due to parasitics neglected during modeling of the system. Now, note that any small disturbance or noise in the system will push the state E off the constraint set $\mathcal{M}_{>0}$, such that the "boundary layer" dynamics (22) will determine whether the state will be attracted or repelled from $\mathcal{M}_{>0}$. From Lemma 4.1, $\mathcal{M}^{\text{stable}}_{>0}$ is exactly the attracting portion of $\mathcal{M}_{>0}$, while initial conditions arbitrarily close to $\mathcal{M}^{\text{unstable}}_{>0}$ — if it exists — will be repelled; see Figure 4. Thus, if we performed a measurement on our system in steady state, we would expect to *never* observe voltages near $\mathcal{M}^{\text{unstable}}_{>0}$. Based on physical grounds, we therefore restrict our attention to $\mathcal{M}^{\text{stable}}_{>0}$. □

In the following, local exponential stability of an equilibrium $E^+ \in \mathcal{M}^{\text{stable}}_{>0}$ refers to the behavior of nearby initial conditions also belonging to $\mathcal{M}^{\text{stable}}_{>0}$, see [30].

Theorem 4.2: **(Existence of High-Voltage Equilibrium for Parallel Microgrids).** Consider the closed-loop system (9) for a parallel microgrid resulting from the quadratic droop controller (7). Define the critical voltage vector $E_{\text{crit}} \in \mathbb{R}^n_{>0}$ and the critical load $Q_{\text{crit}} > 0$ by

$$E_{\text{crit}} \triangleq \left(\frac{E^*_{\text{avg}}}{2} \,;\, W_2 \begin{pmatrix} E^*_{\text{avg}}/2 \\ E^*_I \end{pmatrix} \right), \tag{23a}$$

$$Q_{\text{crit}} \triangleq \frac{1}{4} L_{\text{red}} (E^*_{\text{avg}})^2\,. \tag{23b}$$

The following two statements are equivalent:

(i) **Stable High Voltage Equilibrium:** The closed-loop (9) possesses exactly one locally exponentially stable equilibrium $E^+ \in \mathcal{M}^{\text{stable}}_{>0}$ satisfying $E^+ \gg E_{\text{crit}}$;

(ii) **Load Feasibility:** The load is not overly inductive,

$$Q_0 > -Q_{\text{crit}}. \tag{24}$$

If the above statements are satisfied, E^+ is given by

$$E^+_0 = \frac{E^*_{\text{avg}}}{2} \left(1 + \sqrt{1 + \frac{Q_0}{Q_{\text{crit}}}} \right), \tag{25a}$$

$$E^+_i = \frac{C_i E^*_i + |b_{i0}| E^+_0}{C_i + |b_{i0}|}, \quad i \in \{1, \ldots, n-1\}\,. \tag{25b}$$

Remark 5: **(Interpretation of Feasibility Condition).** Theorem 4.2 gives the necessary and sufficient condition for the existence of a "high" voltage equilibrium. That is, each component of the equilibrium is larger than the corresponding component of the strictly positive vector E_{crit} in (23a). One can verify that (12) and (14) reduce to the scalar values

$$L_{\text{red}} = \sum\nolimits_{j=1}^{n-1} \left(\frac{|b_{j0}| C_j}{|b_{j0}| + C_j} \right) > 0\,,$$

$$E^*_{\text{avg}} = \frac{1}{L_{\text{red}}} \sum\nolimits_{j=1}^{n-1} \left(\frac{|b_{j0}| C_j}{|b_{j0}| + C_j} \right) E^*_j > 0\,,$$

and thus the RPFE (16) reduces to a single quadratic equation. The parametric condition (24) is exactly the classic power flow feasibility result for the modified two-node network of Figure 5 [21, Chapter 2].

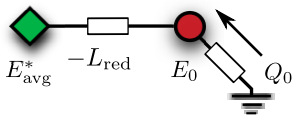

Fig. 5. Single-line equivalent circuit for feasibility condition (24).

Perhaps surprisingly, Theorem 4.2 shows that the voltage stability of parallel networks does not simply decouple line-by-line into $n-1$ voltage stability problems. The critical load (23b) takes into account the network topology, admittances, and droop controller gains, while the ratio Q_0/Q_{crit} serves as an exact security metric for network monitoring. □

Theorem 4.2 establishes the existence and local stability of a high voltage equilibrium for the closed-loop differential-algebraic system (9). From the explicit form of the equilibrium E^+ in (25), the reader may suspect that we have ignored an additional equilibrium. Indeed, under a restricted condition on the load, a "low" voltage equilibrium $E^- \in \mathcal{M}^{\text{stable}}_{>0}$ exists as well. Recall that a hyperbolic equilibrium E^- is said to

be of *type-k* if k of its eigenvalues have positive real parts [19].

Theorem 4.3: **(Unstable Low Voltage Equilibrium for Inductive Loads).** Define the singular load value as

$$Q_{\rm sing} \triangleq \frac{4L_{\rm red}/b_{\rm tot}}{(1+L_{\rm red}/b_{\rm tot})^2} Q_{\rm crit} \in]0, Q_{\rm crit}[\,. \qquad (26)$$

The following two statements are equivalent:

(i) **Unstable Low Voltage Equilibrium:** The closed-loop (9) possesses exactly one hyperbolic type-1 unstable equilibrium $E^- \in \mathcal{M}_{>0}^{\rm stable}$ satisfying $E^- \ll E_{\rm crit}$;

(ii) **Load Restriction :** $Q_0 \in]-Q_{\rm crit}, -Q_{\rm sing}[$.

If the above statements are satisfied, E^- is given by

$$E_0^- = \frac{E^*_{\rm avg}}{2}\left(1 - \sqrt{1+\frac{Q_0}{Q_{\rm crit}}}\right), \qquad (27)$$

with E_i^-, $i \in \{1,\dots,n-1\}$ given by the analog to (25b).

Remark 6: **(Load Restrictions).** The load restriction (ii) ensures that $E^- \in \mathcal{M}_{>0}^{\rm stable}$, c.f. Remark 4. As in Theorem 4.2, no equilibrium E^- exists for $Q_0 < -Q_{\rm crit}$. When $Q_0 = -Q_{\rm crit}$, $E^+ = E^- = E_{\rm crit}$. That is, the stable and unstable equilibria coalesce at value $E_{\rm crit} \in \mathcal{M}_{>0}^{\rm stable}$, then vanish in a saddle-node bifurcation leading to voltage collapse [10], [31]. When $Q_0 = -Q_{\rm sing}$ it holds that $E^- \in \mathcal{S}_{>0}$, and the stability properties of E^- change via a singularity-induced bifurcation [32]. Indeed, when $Q_0 \in]-Q_{\rm sing}, 0[$ one can show that $E^- \in \mathcal{M}_{>0}^{\rm unstable}$. In this regime, E^- is in fact locally exponentially stable, but is unstable in the ambient space for the associated parasitic dynamics, see Figure 4 and Remark 4. For $Q_0 \geq 0$, E^- has negative elements and is therefore not in the state space $\mathcal{M}_{>0}$. □

Taken together, Lemma 4.1 along with Theorems 4.2 and 4.3 give a clear picture of the dynamics on the state space; depending on the problem parameters, there are always either zero, one, or two equilibria in $\mathbb{R}^n_{>0}$ (Figure 4).

V. Revisiting the Conventional Droop Controller

As we have seen, the analysis of a parallel microgrid controlled by the quadratic droop controller (7) is considerably simpler than the analogous but seemingly intractable problem for the conventional droop controller (6). We can in fact leverage the results of Sections III and IV to provide a partial analysis of the conventional droop controller (6). The following result — the proof of which follows by comparing (6) and (7) — relates the equilibria of the two closed-loop systems for a special choice of controller gains.

Lemma 5.1: **(Equilibria of Conventional Droop Controller).** Consider the respective closed-loop systems resulting from the conventional droop controller (6) and the quadratic droop controller (7) for an arbitrary network topology. The following two statements are equivalent:

(i) **Quadratic System:** $E \in \mathcal{M}_{>0}$ is an equilibrium of the quadratic droop-controlled system with controller gains $C_i > 0$, $i \in \mathcal{V}_I$;

(ii) **Conventional System:** $E \in \mathcal{M}_{>0}$ is an equilibrium of the conventionally droop-controlled system with controller gains $\widetilde{C}_i = C_i E_i$ where $C_i > 0$, $i \in \mathcal{V}_I$.

Theorem 5.2: **(Stability of Conventional Droop Controller).** Consider the closed-loop system resulting from the conventional droop controller for a parallel microgrid. Assume that (24) holds, and that the controller gains are chosen as in Lemma 5.1. If

$$\max_{i,j\in\{1,\dots,n-1\}} \frac{E_i^*}{E_j^*} < 2\,, \qquad (28)$$

then E^+, as given by (25), is locally exponentially stable.

The mild extra condition (28) in Theorem 5.2 requires that the inverter voltage set points are sufficiently similar, and in practice is always satisfied.

VI. Simulation of IEEE 37 Bus Distribution Network

While the exact stability results of Section IV hold only for the case of an inductive parallel microgrid, in this section we illustrate the behavior of our quadratic droop controller in a lossy distribution network. Specifically, Figure 6 shows the performance of the controller in a modified version of the IEEE 37 distribution network. After an islanding event, the distribution network is disconnected from the transmission grid, and the (for clarity, identical) distributed generators must take decentralized action to ensure network stability.

At time $t = 3$ seconds, one of the inductive loads in the network doubles, and the voltages at the distributed generators are adjusted according to the quadratic droop controller (7). Thus, the controller stabilizes the network even in the presence of large transfer conductances (high R/X ratio). However, the quadratic droop controller shares one of the drawbacks of the conventional voltage-droop controller; namely, the generators do not equally share the required power demand upon an increase in load (see Section VII).

TABLE I
Controller parameters for IEEE 37 simulation.

Parameter	Symbol	Value
Nom. Voltage	E_i^*	4.8 kV
Quad. Droop Coef.	C_i	0.5 S
Time Constants	τ_i	0.01 s

VII. Conclusions

In this work we have presented and analyzed a novel voltage controller for inductive microgrids. Unlike the conventional droop controller, our proposed quadratic design is physically well motivated, and can be interpreted within "control by interconnection" paradigm. This leads to an elegant circuit-theoretic description of the closed-loop, and to an exact analysis of the network equilibria and their stability properties. The analytical progress in this work now enables a rigorous study of several important and challenging problems. First and foremost, an examination of how to share reactive power demand among heterogeneous generating

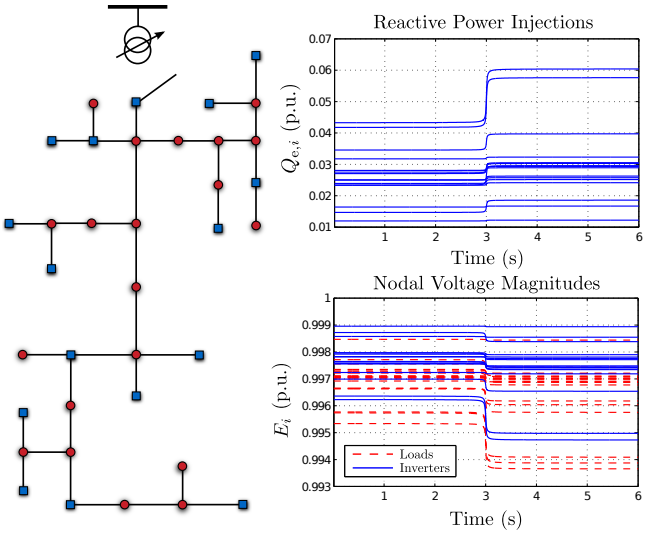

Fig. 6. IEEE 37 bus distribution network containing loads ● and inverters ■, along with simulation results when controlled with the quadratic droop controller (7).

units now seems feasible. Second, with the fundamental case of an inductive microgrid understood, the design of a provably functional decentralized controller for mid-ranged R/X networks is a potentially tractable problem. Third and finally, this work should facilitate the design of so-called "secondary" integral controllers. Although classically used only to eliminate voltage deviations at the distributed generators, these integral controllers could also potentially address the previous two issues of reactive power sharing and elevated R/X ratios.

REFERENCES

[1] J. A. P. Lopes, C. L. Moreira, and A. G. Madureira, "Defining control strategies for microgrids islanded operation," *IEEE Transactions on Power Systems*, vol. 21, no. 2, pp. 916–924, 2006.

[2] J. M. Guerrero, J. C. Vasquez, J. Matas, L. G. de Vicuna, and M. Castilla, "Hierarchical control of droop-controlled AC and DC microgrids–a general approach toward standardization," *IEEE Transactions on Industrial Electronics*, vol. 58, no. 1, pp. 158–172, 2011.

[3] Q.-C. Zhong and T. Hornik, *Control of Power Inverters in Renewable Energy and Smart Grid Integration*. Wiley-IEEE Press, 2013.

[4] A. Tuladhar, H. Jin, T. Unger, and K. Mauch, "Parallel operation of single phase inverter modules with no control interconnections," in *Applied Power Electronics Conference and Exposition*, Atlanta, GA, USA, Feb. 1997, pp. 94–100.

[5] S. Barsali, M. Ceraolo, P. Pelacchi, and D. Poli, "Control techniques of dispersed generators to improve the continuity of electricity supply," in *IEEE Power Engineering Society Winter Meeting*, New York, NY, USA, Jan. 2002, pp. 789–794.

[6] R. Majumder, A. Ghosh, G. Ledwich, and F. Zare, "Power system stability and load sharing in distributed generation," in *Power System Technology and IEEE Power India Conference*, New Delhi, India, Oct. 2008, pp. 1–6.

[7] Y. U. Li and C.-N. Kao, "An accurate power control strategy for power-electronics-interfaced distributed generation units operating in a low-voltage multibus microgrid," *IEEE Transactions on Power Electronics*, vol. 24, no. 12, pp. 2977–2988, 2009.

[8] J. M. Guerrero, J. C. Vasquez, J. Matas, M. Castilla, and L. G. de Vicuna, "Control strategy for flexible microgrid based on parallel line-interactive UPS systems," *IEEE Transactions on Industrial Electronics*, vol. 56, no. 3, pp. 726–736, 2009.

[9] J. W. Simpson-Porco, F. Dörfler, and F. Bullo, "Synchronization and power sharing for droop-controlled inverters in islanded microgrids," *Automatica*, vol. 49, no. 9, pp. 2603–2611, 2013.

[10] I. Dobson, "Observations on the geometry of saddle node bifurcation and voltage collapse in electrical power systems," *IEEE Transactions on Circuits and Systems I: Fundamental Theory and Applications*, vol. 39, no. 3, pp. 240–243, 1992.

[11] J. Machowski, J. W. Bialek, and J. R. Bumby, *Power System Dynamics*, 2nd ed. Wiley, 2008.

[12] Smart Grid Investment Grant Program, "Application of automated controls for voltage and reactive power management - initial results," U.S. Department of Energy, Tech. Rep., Dec. 2012.

[13] M. C. Chandorkar, D. M. Divan, and R. Adapa, "Control of parallel connected inverters in standalone AC supply systems," *IEEE Transactions on Industry Applications*, vol. 29, no. 1, pp. 136–143, 1993.

[14] Q.-C. Zhong, "Robust droop controller for accurate proportional load sharing among inverters operated in parallel," *IEEE Transactions on Industrial Electronics*, vol. 60, no. 4, pp. 1281–1290, 2013.

[15] Z. Wang, M. Xia, and M. D. Lemmon, "Voltage stability of weak power distribution networks with inverter connected sources," in *American Control Conference*, Washington DC, USA, Jun. 2013, pp. 6592–6597.

[16] F. Wu and S. Kumagai, "Steady-state security regions of power systems," *IEEE Transactions on Circuits and Systems*, vol. 29, no. 11, pp. 703–711, 1982.

[17] J. Thorp, D. Schulz, and M. Ilić-Spong, "Reactive power-voltage problem: conditions for the existence of solution and localized disturbance propagation," *International Journal of Electrical Power & Energy Systems*, vol. 8, no. 2, pp. 66–74, 1986.

[18] R. Ortega, A. J. van der Schaft, B. Maschke, and G. Escobar, "Interconnection and damping assignment passivity-based control of port-controlled Hamiltonian systems," *Automatica*, vol. 38, no. 4, pp. 585–96, 2002.

[19] S. Sastry and C. Desoer, "Jump behavior of circuits and systems," *IEEE Transactions on Circuits and Systems*, vol. 28, no. 12, pp. 1109–1124, 1981.

[20] P. Kundur, *Power System Stability and Control*. McGraw-Hill, 1994.

[21] T. Van Cutsem and C. Vournas, *Voltage Stability of Electric Power Systems*. Springer, 1998.

[22] E. C. Furtado, L. A. Aguirre, and L. A. B. Tôrres, "UPS parallel balanced operation without explicit estimation of reactive power – a simpler scheme," *IEEE Transactions on Circuits and Systems II: Express Briefs*, vol. 55, no. 10, pp. 1061–1065, 2008.

[23] B. W. Williams, *Power Electronics: Devices, Drivers, Applications and Passive Components*. McGraw-Hill, 1992.

[24] E. A. A. Coelho, P. C. Cortizo, and P. F. D. Garcia, "Small-signal stability for parallel-connected inverters in stand-alone AC supply systems," *IEEE Transactions on Industry Applications*, vol. 38, no. 2, pp. 533–542, 2002.

[25] M. Dai, M. N. Marwali, J.-W. Jung, and A. Keyhani, "Power flow control of a single distributed generation unit with nonlinear local load," in *IEEE Power Systems Conference and Exposition*, New York, USA, Oct. 2004, pp. 398–403.

[26] M. N. Marwali, J.-W. Jung, and A. Keyhani, "Stability analysis of load sharing control for distributed generation systems," *IEEE Transactions on Energy Conversion*, vol. 22, no. 3, pp. 737–745, 2007.

[27] Y. Mohamed and E. F. El-Saadany, "Adaptive decentralized droop controller to preserve power sharing stability of paralleled inverters in distributed generation microgrids," *IEEE Transactions on Power Electronics*, vol. 23, no. 6, pp. 2806–2816, 2008.

[28] A. J. van der Schaft, "Characterization and partial synthesis of the behavior of resistive circuits at their terminals," *Systems & Control Letters*, vol. 59, no. 7, pp. 423–428, 2010.

[29] F. Dörfler and F. Bullo, "Kron reduction of graphs with applications to electrical networks," *IEEE Transactions on Circuits and Systems I: Regular Papers*, vol. 60, no. 1, pp. 150–163, 2013.

[30] D. J. Hill and I. M. Y. Mareels, "Stability theory for differential/algebraic systems with application to power systems," *IEEE Transactions on Circuits and Systems*, vol. 37, no. 11, pp. 1416–1423, 1990.

[31] I. Dobson and H. C. Chiang, "Towards a theory of voltage collapse in electric power systems," *Systems & Control Letters*, vol. 13, no. 3, pp. 253–262, 1989.

[32] V. Venkatasubramanian, H. Schattler, and J. Zaborsky, "Dynamics of large constrained nonlinear systems-a taxonomy theory," *Proceedings of the IEEE*, vol. 83, no. 11, pp. 1530–1561, 1995.